Pressure Dependent Quality Factor of Micron Scale Single Mass Cantilever Energy Harvesters

Ayoola T. Brimmo[1], Mohamed I. Hassan [*1], Aveek. N. Chatterjee[2]
[1]Mechanical and Materials Engineering Department, Masdar Institute of Science and Technology, Abu Dhabi, UAE
[2]MEMS Department, GLOBALFOUNDRIES, Singapore
*Corresponding author: Masdar Institute P.O.Box 54224, Abu Dhabi UAE; miali@masdar.ac.ae

Abstract: The aim of this study is to predict the extent of damping (measured as Q-factor) of a single mass cantilever energy harvester, at various cavity pressure, using the commercial finite element tool, COMSOL. Varying the pressure from atmospheric to near vacuum conditions, we calculate the Q-factor of the structure due to squeeze film, slide film, and thermo-elastic damping. Our results show that at near vacuum pressure, the air damping (squeeze and slide film) is negligible and, rather, the intrinsic damping of the structure (thermo-elastic damping) predominates. In the transitional region – transition between viscous and molecular flow—squeeze film damping becomes the predominant mechanism and the Q-factor demonstrates a linear response to pressure in the log-log scale. The micro-scale thickness of the cantilever implied a negligible slide film damping between the cantilever arm and the cavity sidewall. In the viscous and vacuum regime – pressures close to atmospheric and vacuum conditions respectively— the Q-factor shows a minimal response to pressure.

Keywords: Damping, Q-Factor, Energy Harvester, Squeeze film.

1. Introduction

For micro-electro-mechanical systems (MEMs) operating in non-vacuum conditions, air damping is the most dominant damping mechanism [1]. Such damping results in a loss of the device performance. The extent of the performance loss is highly dependent on the cavity pressure which dictates the degree to which the oscillating device is damped. This topic has been widely studied with a common aim of reducing the damping effect of the cavity's fluid [2, 3, 4, 5]. Some experimental studies even provide constitutive equations for predicting the effect of air pressure on viscous damping but these relations only apply to a cantilever with its mass evenly distributed across its area [6]. In predicting this phenomenon for complex shaped resonators, the interaction between the ambient fluid and the energy harvester's structure has to be either studied experimentally or computationally. The repetitive nature of optimization studies makes such experimental efforts costly. Similarly, the multi-physics nature of this problem coupled with the device's irregular shape make the analytical modeling approach unfeasible necessitating the use of computational fluid-structural interaction (FSI) models.

There are two approaches to developing FSI models: (1) using a single solver with the fluid and structural governing equations combined in a single matrix (implicit FSI); (2) coupling two different dedicated solvers for the fluid and structural governing equations (explicit FSI). In the first approach, the damping effect of the fluid is implicitly modeled using simplified theories embedded in the structural dynamics solver. In the second approach, the fluid is modeled explicitly using a Navier Stoke's or Molecular Flow model. While the single matrix approach has an advantage of reducing the computational demand due to its simplification, its accuracy does not match up to the explicit modeling of both physics.

In this study, we use COMSOL to model a single mass cantilever energy harvester (see Figure 1) operating within the ambient to vacuum pressure range. The effect of squeeze-film, slide film, and structural damping on the device's Q-factor was investigated at various pressure levels. The anchor loss (another source of damping in MEMS structure) has been neglected in the present study. In COMSOL, we adapt the single matrix approach and validate these results using both approaches on the ANSYS finite element tool. Validation of the modeling parameters was

also performed using experimental data from a single beam energy harvester. The following sections give details on the mathematical models applied in each approach and the respective results obtained.

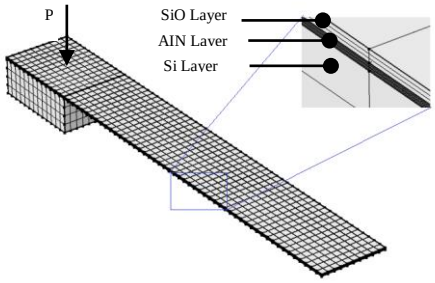

Figure 1: Structure of the modeled MEM energy harvester

2. Numerical Model

The 3D solid mechanics, time dependent solver was used for this study. The Aluminum Nitride (AIN), Silicon Oxide (SiO) and Silicon (Si) layers are all modeled as linear elastic materials. The beam has a total length of 5000µm with a suspended mass length of 1000µm. The thickness of the SiO, AIN and Si layers are 2µm, 1.2µm and 20µm respectively. The thickness of the mass is 390µm. All layers are constrained to be fixed at the opposite end of the mass and a pressure body load is applied on the structure. Thin-film damping loads are applied to the top and bottom boundaries of the structure to model the squeeze film damping, and at the sides of the structure to model slide-film damping (direction tangent to the movement of the structure). The thin-film element is inbuilt in COMSOL, and models viscous fluid flow behavior in small gaps. If this gap is between a fixed surface and a moving structure, the thin-film elements model the effect of a squeeze/slide film between the fixed surface and the moving structure. The element behavior is based on the Reynolds squeeze film theory, and the theory of rarefied gases, which are the theoretical background for analyzing fluid structural interaction for microstructures [7, 8]. This approach allows avoidance of an explicit Computational Fluid Dynamics (CFD) model, while modeling squeeze film damping of MEM cantilever.

Wall spacing of 100µm and 140µm are applied for the squeeze and slide film damping boundary loads respectively. The regime of flow is estimated using the Knudsen number (Kn $=\lambda_0 / h$) [9] . At high pressures (Kn < 0.1), the flow is in the continuum region and hence modeled using the Reynolds equation for compressible gas with the non-slip walls approximation:

$$\frac{\partial}{\partial t}(\rho h) + \nabla_t.(h\rho v_{av}) = 0 \qquad (1)$$

Where, λ_0 is the mean free path, ρ is the fluid density, h is the distance between the two plates and v_{av} represents the mean velocity of the flow in the reference plane. v_{av} for the no-slip boundary condition (slip length of the resonator's wall (l_{sw}) and cavity's base (l_{sb}) are both 0) is defined as the combination of the Couette and Poiseuille flow as follows:

$$v_{av} = \frac{1}{2}(v_{w,t} + v_{b,t}) - (h/12\,\mu)\,\nabla_t.P_f \qquad (2)$$

Where, P_f is the fluidic flow pressure, μ is the fluid's viscosity and, $v_{w,t}$ and $v_{b,t}$ are the resonator's wall and cavity's base velocity respectively.

For low pressure regimes (Kn >0.1), equation 1 is modified, by assuming the fluid abides by the ideal gas law, and the total pressure is $P_{tot} = P_a + P_f$ (where P_a is the atmospheric pressure), to the following:

$$\frac{\partial}{\partial t}(P_{tot}h) + \nabla_t.(hP_{tot}v_{av}) = 0 \qquad (3)$$

In this regime, the flow's velocity cannot be treated using the continuum Navier Stokes. Thus, the linearized Boltzmann equation for isothermal flow is utilized. From the solution of the Boltzmann equation, although the slip boundary condition is fundamental to the flow of rarefied gasses, the Couette contribution to the bulk fluid velocity is similar to that of the no-slip condition ($\frac{1}{2}(v_{w,t} + v_{b,t})$). However, in this pressure range, Poiseuille contribution to the fluid's average velocity is handled by the approach of

Fukui and Kaneko [10] which uses an empirical fit to the flow to deduce the fluid's average velocity as:

$$v_{av} = \frac{1}{2}\left(v_{w,t} + v_{b,t}\right) - \left(\frac{h^2}{12\mu_{eff}}\right)\nabla_t . P_f \qquad (4)$$

Where, μ_{eff} is the fluid's effective dynamic viscosity, which according to Veijola [11] is estimated as:

$$\mu_{eff} = \frac{\mu}{1+9.638Kn^{1.159}} \qquad (5)$$

This treatment of μ_{eff} is known in the COMSOL platform as the Rarefied Total Accommodation. Dynamic viscosity (μ) and Mean Free Path (Λ_0) values of 1.85e-5Pa.s and 68nm were used respectively. It is important to note that, for squeeze film, only Normal-pressure forces were considered, while only Couette forces were considered for the slide film model.

Thermo-elastic damping was taking into account by coupling a thermo-elasticity terms – derived from the first law of thermodynamics to the Solid Mechanics interface. This is enabled by including a heat source term in the standard energy equation which couples the heat transfer problem with the structural problem and vice versa [12]

To validate our modelling approach and boundary conditions, we intially modeled the experimental setup of Pandey and Pratap [3] to compare experimetnal results with our calculations. To ensure that numerical damping was avoided, prior to setting up the squeeze, slide and thermo-electric damping loads, the beam was set to oscilate with, a strict time stepping criteria and a tolerance of 0.001.

Upon validating our model, the displacement-time response of the resonator is calculated with the pressure varying from near vacuum to ambient conditions. From this response, we define the logarithmic decrement (δ) using the ratio of two peak heights, $y(t_n)$, seperated by n succesive cycles of period T [13]:

$$\delta = \frac{1}{n}\ln\frac{y(t_n)}{y(t_{n+nT})} \qquad (6)$$

The damping ratio ς is then estimated from δ using the following formulae:

$$\varsigma = \frac{\delta}{\sqrt{4\pi^2+\delta^2}} \qquad (7)$$

The effect of pressure variation on the damping of the beam is then estimated using the Q factors which is calculated as:

$$Q = \frac{1}{2\varsigma} \qquad (8)$$

The calculated pressure dependent Q factors are compared with estimates from ANSYS using both implicit and explicit FSI calculations.

3. Results

Figure 2 shows the time domain response of the beam oscillating in the absence of any damping load using different order of magnitudes of the backward differential formulas (BDF). In the absence of damping loads, the resonator is expected to oscillate indefinitely with a constant amplitude. It can be observed that this is not the case using the 1st and 3rd order BDF. In both cases, there seem to be a damping of the resonator. This damping can be called "numerical damping" as it is solely due to the truncation of the BDF at lower order of magnitudes. It would be misleading to use lower order BDFs to model the squeeze, slide, and thermo-elastic damping as this numerical damping would be wrongfully attributed to the viscous or material damping.

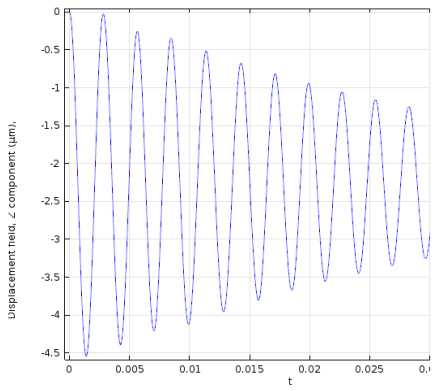

(a) 1st order BDF (Default)

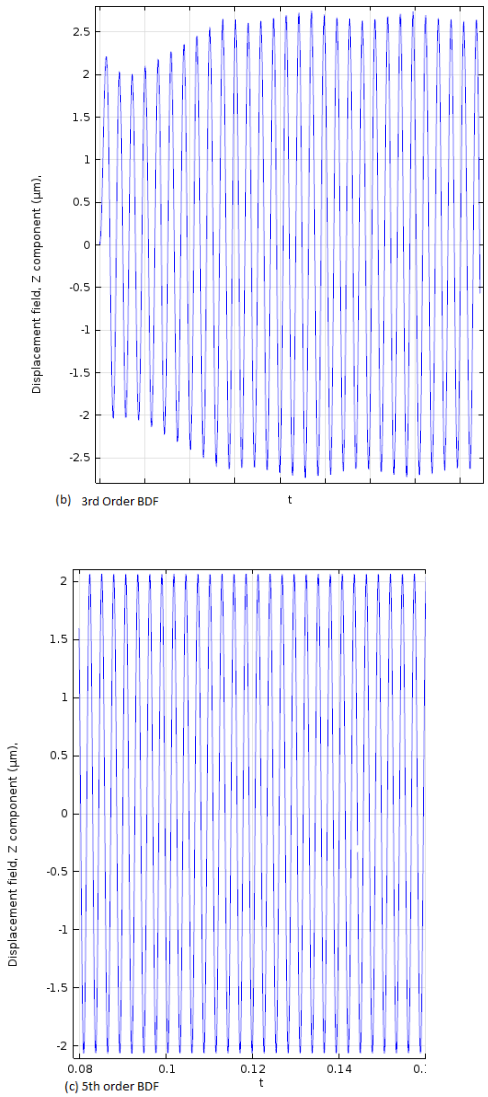

Figure 2: Effect of BDF order on Numerical damping

Modeling the cantilever resonators adapted by Pandey and Pratap [3], we replicate their experimental results to investigate the effect of cantilever length on the device's first mode Q–factor. Figure 3 shows a good agreement (maximum of 3% deviation) between the measured and calculated results, which validates our modeling approach.

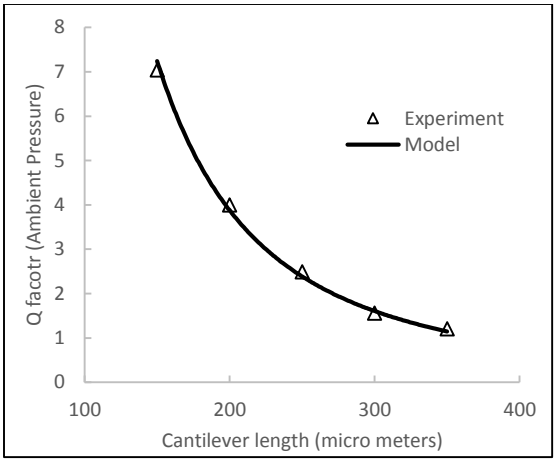

Figure 3: Modeling technique validation: effect of cantilever length on Q factor

Similarly, Table 1 shows that our calculated Q-factors for the first three modes of the cantilever resonator [3] are in good agreement with our model's estimates of same. A maximum deviation of 6% was observed at the 3rd mode. This suggests the fitness of our methodology in performing Q factor calculations up to the third mode.

Table 1: Q factor of first three modes

	Model's Q Factor	Measured Q Factor	Q Factor Error
First Mode	1.21	1.20	1%
Second Mode	7.92	7.58	5%
Third Mode	19.55	18.52	6%

To ensure our results are independent of the computational grid size, mesh sensitivity analyses were performed. The modal frequencies and Q factor were estimated while the grid size was increased from 10 elements to 100000 elements. Figure 4 shows that the modal frequency results converge at about 500 elements, and increasing the number of elements above this value does not affect the calculated modal frequencies.

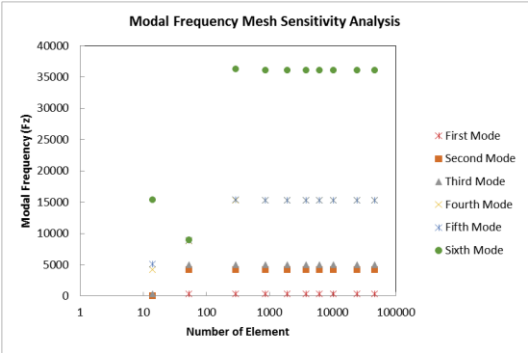

Figure 4: Mesh sensitivity analysis for present's study energy harvester: Modal Frequency

However, Figure 5 shows that a higher number of elements are required for the Q factor convergence. Hence, for studies focused on predicting damping, it would be misleading to perform the mesh sensitivity analysis based on the modal frequencies. Similarly, Figure 6 and Figure 7 demonstrate the dependence of the first mode frequency and Q factor on the utilized time step. Again, it is observed that the first mode frequency converges before the Q factor. The accuracy of a resonator's transient model is highly dependent on the time step utilized as this dictates the ability of the model to catch certain frequencies of oscillation.

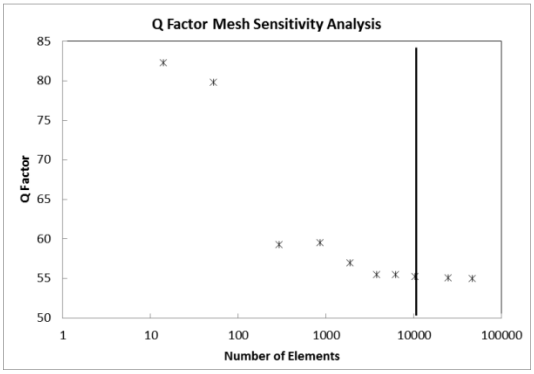

Figure 5: Mesh sensitivity analysis for present's study energy harvester: Q factor

If the time step is greater than the inverse of the first modal frequency, no oscillation is captured by the transient model. Hence, the model is incapable of estimating the modal frequency or the Q factor. As the time step is reduced, the device's oscillation is progressively captured. However, the accuracy of the transient response's amplitude is also highly dependent on the resolution of the time points. If the time step utilized is not small enough to capture the exact peak, an extrapolated peak is used to estimate Q factor. Further reducing the time-step affects the computed Q factor. Figure 7 demonstrates this trend of further increment of Q factor with a reduction in time step below the converged frequency time step. However, we observed from our study that Q-factor convergence is attained when a time step less than $\boldsymbol{T_1/2000}$ is used. Where: $\boldsymbol{T_1}$ is the period of the first mode frequency.

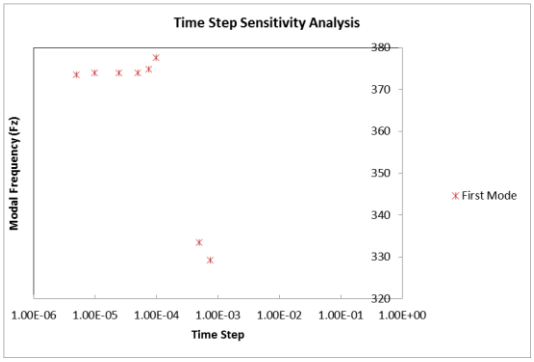

Figure 6: Time step sensitivity analysis for present's study energy harvester: Modal Frequency

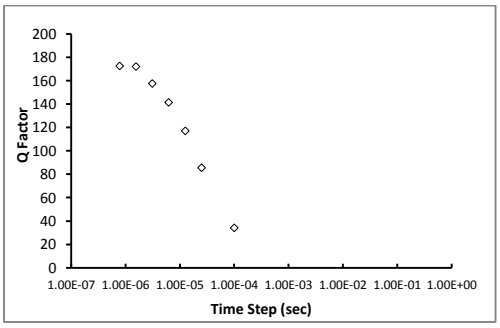

Figure 7: Time step sensitivity analysis for present's study energy harvester: Q factor

Figure 8 shows the effect of varying the cavity pressure on the resonator's Q factor. Between 0.00001-0.001 Torrs, the device's Q factor is observed to be independent of cavity pressure. It is believed that at such low pressure, the air damping is negligible. Therefore, further reduction in air pressure has no significant effect on damping. The high Q factor at such pressure suggests that the intrinsic (thermo-elastic) damping is dominant in this region. As thermo-

elasticity is not dependent on pressure, the Q factor in this region is not expected to be dependent on pressure.

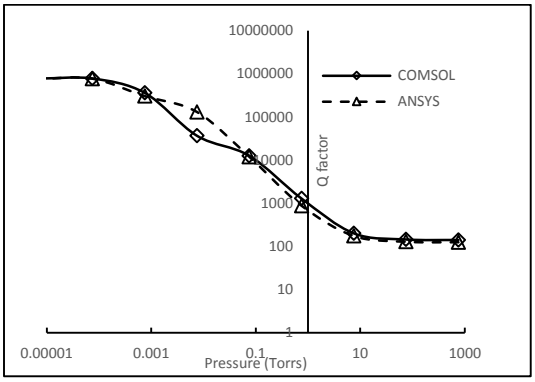

Figure 8: Q factor as a function of cavity pressure.

As the cavity pressure increases above 0.001 Torrs, air damping becomes a dominant mechanism. However, at 0.001 Torrs the air molecules are still sparsely populated in the cavity and little or no interaction between these molecules is expected. As the pressure increases, interaction between air molecules increases which increases the structure's damping. At pressure levels above 10 Torrs, air molecules are now densely packed and viscous. As viscosity is not dependent on pressure, the Q factors above this pressure do not vary significantly with pressure. This result suggests that three different regions exist between vacuum pressure and ambient conditions, which correlates with previous experimental studies [6].

Furthermore, Figure 8 shows a good agreement between estimates from COMSOL and ANSYS using the implicit FSI approach. The explicit FSI approach was also considered in ANSYS and only a 7% deviation in the computed Q factor was observed at ambient pressure. However, the computational time is 15 times more than that required for the implicit FSI approach in both COMSOL and ANSYS. As ANSYS does not currently have a molecular flow model in its fluid dynamics package (Fluent), pressure reduction could not be modeled using the explicit FSI approach. COMSOL's explicit FSI approach has also proven to be computationally costly when the transient study is used. Currently, a frequency domain study is not available in COMSOL's fluid dynamics package. It is suggested that development in this domain should be considered as this could reduce the computational time for such explicit FSI computations. Approximating the relatively thin AIN and SiO layers by using a single Si layer with an effective modulus also proved to be helpful in reducing the computational cost of the explicit FSI approach.

4. Conclusions

In this study, we have used COMSOL to predict the extent of damping (measured as Q-factor) of a single mass cantilever energy harvester, at various cavity pressure. Model validations were performed using experimental data. Mesh and times step sensitivity analyses showed that the modal frequencies converges quicker than the Q factor. Our results suggest that squeeze film damping dominates at high pressure while the thermo-elastic damping is dominant at low pressures. The micro-scale thickness of the cantilever and relatively large side wall gap implied a negligible slide film damping between the cantilever arm and the cavity sidewall. In the viscous and vacuum regimes – pressures close to atmospheric and vacuum conditions respectively — the Q-factor shows a minimal response to pressure.

5. Acknowledgements

This work was funded by Mubadala Development Company (Abu Dhabi), Economic Development Board (Singapore), and GLOBALFOUNDRIES (Singapore) under the framework of 'Twinlab' project with participation of A*STAR Institute of Microelectronics - Singapore, Masdar Institute of Science and Technology - Abu Dhabi, and GLOBALFOUNDRIES - Singapore.

6. References

[1] H. Hosaka, K. Itao and S. Kuroda, "Damping characteristics of beam shaped micro-oscillators," *Sensor Actuators A*, vol. 49, pp. 87-95, 1995.

[2] A. Roychowdhury, A. Nandy, C.S. Jog and

R. Pratap, "A monolithic, FEM based approach for coupled squeeze film problem of an oscillating elastic micro-plate using 3D 27- node elements," *Journal of Applied Mathematics and Physics* , vol. 1, pp. 20-25, 2013.

[3] A.K. Pandey and R. Pratap, "Effect of lfexural modes on squeeze film damping in MEMs cantilever resonators," *Journal of Micromechanics and Microengineeering* , vol. 17, pp. 2475-2484, 2007.

[4] M.Li, H.X. Tang and M.L. Roukes, "Ultra sensitive NEMs based cantilever for sensing, scanned probe and very high frequency applications," *Natur Nanotechnology*, vol. 2, pp. 114-120, 2007.

[5] R. B. Darling, C. Hivick and J. Xu, "Compact analytical modeling of squeeze film damping with arbitrary venting conditions using Green's function approach," *Sensors and Actuators A*, vol. 70, pp. 32-41, 1998.

[6] W.E. Newell, "Minaaturization of Tuning Forks," *Science*, vol. 161, pp. 1320-1326, 1968.

[7] J.J. Blech, " On Isothermal Squeeze Films," *Journal of Lubrication Technology*, vol. 105, pp. 615-620, 1983.

[8] W.E. Langlois, "Isothermal Squeeze Films," *Quarterly Applied Mathematics*, vol. 20, no. 2, pp. 131-150, 1962.

[9] G.A. Bird, Molecular Gas Dynamics and Direct Simulation of Gas Flows, Oxford: Oxford University Press, 1996.

[10] S. Fukui and R. Kaneko, "Analysis of ultra thin gas film lubrication based on the linerized Boltzmann equation: First report -- derivation of a generalized lubrication equation including thermal creep flow," *Journal of Tribology*, vol. 110, no. 2, pp. 253-261, 1988.

[11] T. Veijola, H. Kuisma and J. Lahdenpera, "Equivalent circuit model of the squeezed gas film in a silicon accelerometer.," *Sensors and Actuators A*, vol. 48, pp. 239-248, 1998.

[12] C.J. Adkins, Equilibrium Thermodynamics, Cambridge: Cambridge University Press, 1983.

[13] S.S. Rao, Mechanical Vibration, New York: Wesley, 1995.

[14] P. Kohnke, "Theory Reference for Mechanical APDL and Mechanical Applications," ANSYS, Inc, Canonsburg PA, 2009.